Chapter 3

A restaining method to restore faded fluorescence in tissue specimens

André Huisman, Lennert S. Ploeger, Hub F.J. Dullens,
Jan T.C. Beekhuis, Paul J. van Diest

Submitted for publication

ABSTRACT

The aim of this study was to develop a procedure to remove the TO-PRO-3 fluorescent dye from tissue sections and restain with TO-PRO-3, still allowing calculation of 3-D cellular DNA content and nuclear chromatin texture features by confocal laser scanning microscopy. After staining adrenal tissue with TO-PRO-3 and image acquisition, three destaining approaches were tested based on incubation at different temperatures for different durations in the medium that is normally used to dissolve TO-PRO-3. The same areas were imaged again to measure residual fluorescence, the slides were then restained with TO-PRO-3 and imaged again. After image matching, the grey-values of the images acquired after initial and restaining were compared. A number of 3-D texture features computed after segmentation of nuclei were compared as well. The best destaining result was obtained by incubation of sections at 37°C in pre-heated medium twice for 20 minutes. On average, the 3-D feature values did not change much after de/restaining, except for some discrete texture features which are sensitive to contrast that was slightly lower after restaining.

In conclusion, we present a protocol to remove TO-PRO-3 fluorescence from tissue sections that can subsequently successfully be restained with minimal influence on fluorescence intensity and nuclear chromatin distribution that allows repeated and reliable TO-PRO-3 fluorescence quantification (and probably other intercalating fluorescent dyes) on the same section.

INTRODUCTION

Assessment of nuclear DNA content and nuclear texture features by image analysis has proven to provide diagnostic and prognostic value in tumors from different sites[1,2]. Confocal Laser Scanning Microscopy (CLSM) presents the opportunity to perform 3D DNA content measurements on intact cells in thick histological sections[3]. This has major advantages over the established techniques of flow cytometry and conventional 2-D image cytometry on cytospins: dissociation of tissue with consequently loss of tissue architecture is not required, and inaccuracies caused by cutting or overlap as present in conventional image cytometry on thin tissue sections is almost completely avoided[4, 5]. In a previous study we have described the development of an optimal tissue processing technique for 3-D CLSM used to establish the DNA ploidy[6]. As a measure of histogram quality, the coefficient of variation of the diploid peak was assessed. In addition, we have recently developed implementations to calculate nuclear chromatin texture features in 3-D [7]. We showed the clinical relevance of measuring such 3-D nuclear chromatin texture to discriminate between benign and malignant cell nuclei from prostate cancer tissue [8], and established racial differences in nuclear chromatin distribution patterns between prostate cancer cells from Caucasian and Afro-American men (Chapter 6).

In all these studies, TO-PRO-3 was used for fluorescence staining as it provides optimal specific and quantitative staining of DNA which is quite stable[9, 10]. However, even TO-PRO-3 fluorescence does not remain constant in time due to bleaching and fading, and sometimes the staining fails for different reasons. This means that if several measurements are needed on the same tissue section, one has to choose different imaging areas which makes comparisons more difficult. If staining was not satisfactory, it needs to be repeated which may not be possible if the tissue concerns valuable clinical material or unique structures only present in one slide. It would therefore be of great value to be able to remove the fluorescent dye and restain the specimen without loss of staining quality. Successful removal and restaining of the DNA-bound intercalating dyes propidium iodide (PI) and 7-aminoactinomycin D (7AAD) using methylxanthine caffeine has been reported previously[11]. For TO-PRO-3, a dye with many advantages over PI and 7AAD, such procedures have not been described yet. The aim of this study was therefore to develop a procedure to remove the TO-PRO-3 fluorescent dye from tissue sections and to subsequently restain with TO-PRO-3. The procedure should not harm the calculation of quantitative 3-D DNA and nuclear chromatin texture features on cell nuclei acquired by CLSM. This would allow repeated measurements of fluorescence on the same tissue sections and prevents loss of sections from valuable clinical samples when staining or imaging has initially failed.

MATERIALS AND METHODS

Initial tissue preparation

Fourteen micron thick sections were cut from a representative paraffin-embedded tissue block of adrenal tissue. Our previously developed protocol[6] was used for the initial staining: incubation with RNase-A for 1 hour and staining with the stoichiometric dye

TO-PRO-3 (Molecular Probes, Eugene, OR, USA) iodide (633 nm excitation, maximum emission at 661 nm) in a concentration of 1:2200 for 2 hours at room temperature. TO-PRO-3 was dissolved in a medium containing distilled water, PBS and 0.1 N HCL, further denoted "the medium". After rinsing with distilled water the tissues were mounted in Vectashield (Vector Laboratories, Burlingame, CA, USA) and sealed with a coverslip using nail polish.

Image acquisition and analysis

Image stacks were acquired with a confocal microscope (TCS SP2 AOBS, Leica Microsystems, Heidelberg, Germany) fitted with ×40/1.25 NA oil immersion objective. By adjusting the amplitude of the scanning mirrors an additional zoom factor of 1.5 was established (total magnification of ×60). The depth information was oversampled to obtain (almost) square voxels. Resolution at the specimen level was 0.488 x 0.488 x 0.487 μm^3 and the dynamic range was 12 bits. Six image stacks were acquired to obtain a representative sample from the tissue. The distance between the image stacks was 100 μm to avoid potential bleaching of neighboring fields during image acquisition. The x-y coordinates of each field were stored using in-house developed add-on software for the confocal microscope. These coordinates were used for automated acquisition of the defined fields and were stored for the acquisition of image stacks at the same positions after washing out the fluorescent dye (see below). The bottom and top of the defined fields were identified interactively as the slices where the number of (cut) nuclei was very low[12]. Stacks of approximately 120 2-D digital images (512x512 pixels) were obtained, depending on the effective thickness of the tissue.

Washing out fluorescence and restaining

After initial staining and image acquisition as described above, the coverslip seal was removed using aceton. Next, the slide was incubated in PBS for 1 minute at RT to remove the coverslip and the Vectashield mounting medium. After these steps the specimen was incubated in the medium described above. Three approaches were tested in parallel to find the optimal procedure for removing the fluorescent dye (Table I). In the first approach the tissue was incubated with fresh medium twice for 15 minutes at 37°C. In the second approach the tissue was incubated with fresh pre-heated medium (37°C) twice for 15 minutes at 37°C. The third approach comprised incubation with fresh pre-heated medium (37°C) twice for 20 minutes at 37°C.

After rinsing with distilled water the specimens were again mounted in Vectashield and resealed. Next, image stacks were acquired at the same position in the tissue as the

Table I: Destaining protocols

	Incubation medium	Temperature of incubation medium	Incubation
First protocol	distilled water, PBS, 0.1 N HCL	Room temperature	Twice 15 minutes at 37°C
Second protocol	idem	37°C	Twice 15 minutes at 37°C
Third protocol	idem	37°C	Twice 20 minutes at 37°C

Different protocols that were compared for their ability to remove TO-PRO-3 fluorescence from tissue sections.

initial scan by retrieving the stored locations of the previously acquired image stacks. The residual fluorescence was assessed visually by seeking nuclear structures. For this purpose also a grey level graph of a profile line at the middle slice in a representative image stack was displayed.
After image acquisition the specimen was restained using the above described procedure. Next, image stacks were acquired for the second time using the same settings of the confocal microscope with respect to the PMT settings, size of the pinhole, number of slices and voxel dimensions.

Image matching and comparison

Although the image stacks were acquired at the same slide position using stored x-y coordinates, minute movements and rotation of the microscope stage preclude by definition exact matching of images at the acquired locations. To enable calculating ratios of grey-values for corresponding pixels and to compare individual nuclei, an image matching algorithm was developed. To reduce bias in the direct pixel comparison, a threshold was applied first to remove background noise (grey-values < 20). In addition, downsampling of the image was performed in all 3 dimensions using nearest neighbor interpolation to reduce background noise. We implemented a matching algorithm using the open source Image Processing ToolKit (ITK, Kitware Inc., New York, USA). Affine transforms (translation, rotation and scaling) were applied to the images until the images matched. For an optimal search through all different possible affine transforms, the simplex method was used for guiding this optimization process[13]. A normalized correlation metric was used as the cost function for matching and was computed after each affine transform. Optimization was stopped when the parameters of the affine transform or the cost-function converged to a stable solution (when the difference in cost function value and parameters of the affine transform were less than 0.01).
After image matching, the intensity of the images acquired after restaining were compared with the intensity of the images acquired after the initial staining by computing the average grey-values, sum of grey-values and the standard deviation of the grey-values. To verify that restaining of the specimen would give reproducible results with respect to the initial staining, nuclei were segmented as well, applying our previously described procedures for segmentation[12]. Subsequently, 3-D texture features were computed [7]. For all nuclei, the ratios between the initial and restaining feature values were computed.

RESULTS

Figure 1 shows the initial fluorescence, residual fluorescence after destaining and restaining results for the 3 protocols (center image of the 3-D stack). It appears that TO-PRO-3 fluorescence was only completely removed by the third protocol. The matching algorithm applied to the initial image and the restaining image for the third protocol finished after on average 242 iterations for the 3 protocols with a correlation between the images between -0.93 and -0.95. Table II shows the results of the comparison between the fluorescence intensities calculated from initial staining and after destaining/restaining with the three protocols. The average grey-value showed a decrease of 0.5% for the first,

Table II: Fluorescence intensity after restaining.

Staining procuedure	Sum of grey-values (×10^6)	Mean grey-value	SD of grey-values	Average texture feature ratio	SD of texture feature ratios
Protocol 1					
Initial staining	1441	405	474	1.12	0.31
Final staining	1433	403	486		
Protocol 2					
Initial staining	1995	334	464	1.30	1.20
Final staining	1912	320	307		
Protocol 3					
Initial staining	989	209	293	1.02	0.43
Final staining	970	205	209		

Analysis of fluorescence intensity differences by quantitative 3-D confocal microscopy between the images after initial TO-PRO-3 staining compared to the images acquired after destaining and restaining of adrenal tissue for the 3 destaining/restaining protocols. SD = standard deviation.

4.3% for the second and a decrease of 2.0% for the third protocol.

Table III shows the computed ratios between the values obtained after the initial and restaining for a number of grey-value distribution characteristics and 3-D nuclear texture features for the three protocols. These ratios were computed for all segmented and matched nuclei. The sum of grey-values decreased on average 6% for the first, 24% for the second and 25% for the third protocol. The overall average of the average ratios for all features was 1.1 (SD 0.31) for the first, 1.3 (SD 1.2) for the second and 1.0 (SD 0.43) for the third protocol. The highest variation was seen for the discrete texture features.

DISCUSSION

Due to fading and bleaching of fluorescence, it is difficult to repeat fluorescence measurements for quantitative image analysis. To overcome this, we developed a procedure to remove TO-PRO-3, a popular stoichiometric fluorescent dye, from tissue sections and to restain them with TO-PRO-3. We previously showed that TO-PRO-3 staining is possible for various tissues[8]. Although we only used adrenal tissue in the present study as a model, we expect this technique to work on other tissues as well. Adequate destaining is critical, as residual dye that may (partially) have lost its fluorescent properties will hinder binding of fresh dye, thereby negatively influencing stoichiometry and quantification.

Destaining was done with the medium normally used for dissolving TO-PRO-3, containing distilled water, PBS and 0.1 N HCL. Pre-heating the medium at 37°C appeared to remove the fluorescent dye to a larger extent, and after incubating the tissue twice for 20 minutes at 37°C the TO-PRO-3 fluorescence disappeared almost completely. This pre-heating step corresponds to a longer incubation time at the same temperature, but we prefer preheating the medium to minimize incubation of the sections in different solutions that may in the end perhaps damage the tissue. Because of hydrolysis which occurs due to the presence of HCl in the medium, the DNA unfolds and the binding of the TO-PRO-3 molecules to the minor groove of the DNA is disconnected. Hydrolysis occurs at a higher

Table III. Changes in texture features after restaining for the different protocols

	Protocol 1		Protocol 2		Protocol 3	
3-D feature	Average ratio	SD	Average ratio	SD	Average ratio	SD
Grey sum	0.94	0.06	0.76	0.03	0.75	0.03
Grey mean	0.94	0.06	0.76	0.03	0.75	0.03
Grey variance	1.03	0.16	0.51	0.08	0.53	0.08
Grey skewness	1.13	0.16	1.25	0.47	1.10	0.47
Grey kurtosis	1.10	1.99	1.25	0.40	1.09	0.40
Energy	1.23	0.34	1.30	0.19	1.64	0.19
Entropy	0.98	0.04	1.08	0.04	0.97	0.04
Inverse difference moment	1.10	0.16	0.94	0.07	1.31	0.07
Inertia	1.06	0.22	0.96	0.08	0.60	0.08
Correlation	0.82	0.25	0.30	0.06	0.32	0.06
Cluster shade	1.20	0.40	0.43	0.68	0.46	0.68
Cluster prominence	1.20	0.39	0.30	0.32	0.34	0.32
Low dens. pixel volume	1.02	0.16	0.98	0.11	1.04	0.11
Med. dens. pix. vol.	0.99	0.03	1.04	0.02	1.00	0.02
High dens. pix. vol.	0.99	0.03	0.92	0.04	0.98	0.04
Low avg.ext.rat.	0.91	0.16	1.46	0.18	1.16	0.18
Med avg.ext.rat.	0.99	0.02	1.06	0.02	1.01	0.02
High avg.ext.rat.	1.03	0.05	0.91	0.03	0.96	0.03
Low vs. medium avg. ext. rat	1.12	0.12	0.75	0.09	0.92	0.09
Low vs. med-high average extinction ratio	1.16	0.14	0.74	0.11	0.91	0.11
Low vs. high avg. ext. rat.	1.18	0.15	0.73	0.12	0.90	0.12
Number of unconnected low areas	1.93	1.66	3.36	1.69	2.67	1.69
Number of unconn. med. areas	2.35	1.94	1.33	0.77	1.23	0.77
Number of unconn. high areas	1.55	0.92	6.77	0.93	1.54	0.93
Low compactness	0.51	0.22	1.00	0.19	0.56	0.19
Med compact.	1.29	0.15	2.55	0.18	1.35	0.18
High compact.	1.46	0.28	3.96	0.30	1.65	0.30
Low avg. dist. geo-center	0.98	0.04	1.00	0.02	0.98	0.02
Med avg. dist. geo-center	1.00	0.01	0.99	0.01	1.00	0.01
High avg.dist. geo-center	1.04	0.04	1.06	0.03	1.01	0.03
low asym.nuc.cntr	1.07	0.58	1.15	0.15	0.98	0.15
med asym.nuc.cntr	1.01	0.03	0.96	0.02	1.01	0.02
high asym. nuc. Cntr	1.01	0.03	1.09	0.04	1.03	0.04
Lacunarity	0.92	0.08	0.92	0.07	0.95	0.07
Fractal dimension	1.00	0.01	1.01	0.01	1.00	0.01
Average	1.12	0.32	1.30	0.22	1.02	0.43
Standard deviation	0.31		1.2		0.43	

Average ratios (and standard deviations (SD)) of grey-value distribution features and 3-D nuclear chromatin texture features computed by confocal microscopy on segmented and matched nuclei after initial TO-PRO-3 fluorescence staining, destaining and restaining of adrenal tissue. The ratios are computed from the features computed per nucleus on the final fluorescence signal, divided by the feature values of the nuclei obtained after the initial staining.

rate at a temperature of 37°C, which explains the better effect of the preheated medium. This protocol (protocol 3) is therefore optimal when it is important to completely remove the dye, e.g. when restaining with an other dye will follow.
After restaining, image acquisition at the same location in the slide based on stored x-y coordinates and matching of the correct image regions, grey-value ratios were computed for all overlapping pixels. The average grey-value ratio, computed per pixel, showed for the third protocol a decrease in image intensity of 12% for the third protocol (2x20 minutes destaining in preheated medium). The standard deviation of the ratios was 0.33, which seems rather high, but is probably largely caused by imperfect image matching. When taking the nuclei into account there was an average decrease in image intensity of 25%. Although there was a certain reduction in the fluorescence intensity, this will be in practice easily compensated for by increasing the PMT voltage resulting in higher intensities. Because the sum of grey values computed for each individual nucleus does not increase, the global increase in intensity after restaining with Protocol 1 is probably caused by imperfect matching and more background signal. Protocol 1 and 2 also gave satisfactory results after restaining, although their destaining ability was less. This can probably be explained by the fact that when restaining, the sections are incubated again in the medium for 2 hours (although at RT) which will further destain the slides. Because the slides were quickly processed after imaging, the residual TO-PRO-3 may not have lost its fluorescent properties as well.
On average, the 3-D feature values did not change much between calculations on the nuclei segmented from images acquired after initial staining and the nuclei obtained from the restained image stacks. However, due to the lower contrast in the image stacks acquired after restaining, the values for some texture features differ from their values after initial staining, especially for the discrete texture features which are sensitive to contrast. Previous studies have shown that these features may be clinically relevant[8]. Due to their sensitivity to slight contrast changes, one should ensure that the images under consideration have comparable contrast properties. These features are otherwise not considered to be stable features for clinical classification purposes.
Although the number of segmented nuclei did not allow sensible DNA ploidy calculations, ploidy measurements will not likely be influenced by the restaining procedure, since the sum of grey-values, a measure for the amount of DNA, decreases linearly in all voxels and thereby all nuclei since the standard deviation for this feature is only 0.03. Proper measurements of DNA ploidy on restained images should therefore be well possible.
In conclusion, we presented a protocol to remove TO-PRO-3 fluorescence from tissue sections that can subsequently successfully be restained with minimal influence on fluorescence intensity and nuclear chromatin distribution. This protocol allows repeated and reliable TO-PRO-3 fluorescence quantification on the same section. It is likely that this procedure will also work for other intercalating fluorescent dyes.

Figure 1: Effect of different fluorescence destaining/restaining protocols imaged by confocal microscopy. (a) initial fluorescence of adrenal tissue stained with TO-PRO-3 (b) same area after incubation in destaining medium for 2x15 minutes at 37°C.(c) same area after restaining. (d), (e) and (f) show the intensity profiles of the indicated central lines in (a), (b) and (c), respectively.
(g) initial fluorescence of adrenal tissue stained with TO-PRO-3. (h) same area after incubation for 2x15 minutes at 37°C in pre-heated (37°C) destaining medium. (i) same area after restaining. (j), (k) en (l) show the intensity profile of the indicated central lines in (g), (h) and (i), respectively.
(m) initial fluorescence of adrenal tissue stained with TO-PRO-3. (n) same area after incubation for 2x20 minutes at 37°C in pre-heated (37°C) destaining medium. (o) same area after restaining. (p), (q) en (r) show the intensity profile of the indicated central lines in (m), (n) and (o), respectively.

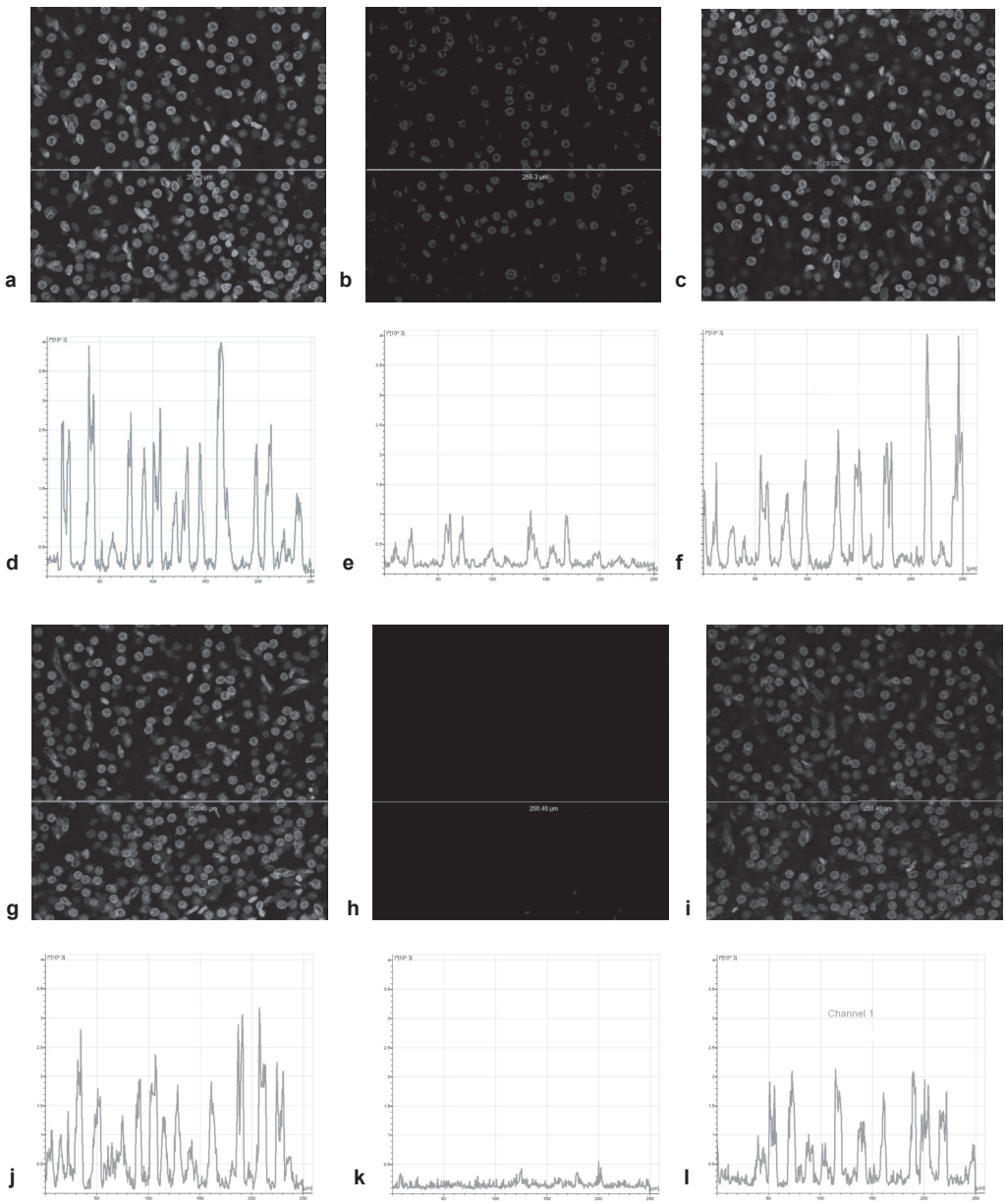

Figure 1 (continued)

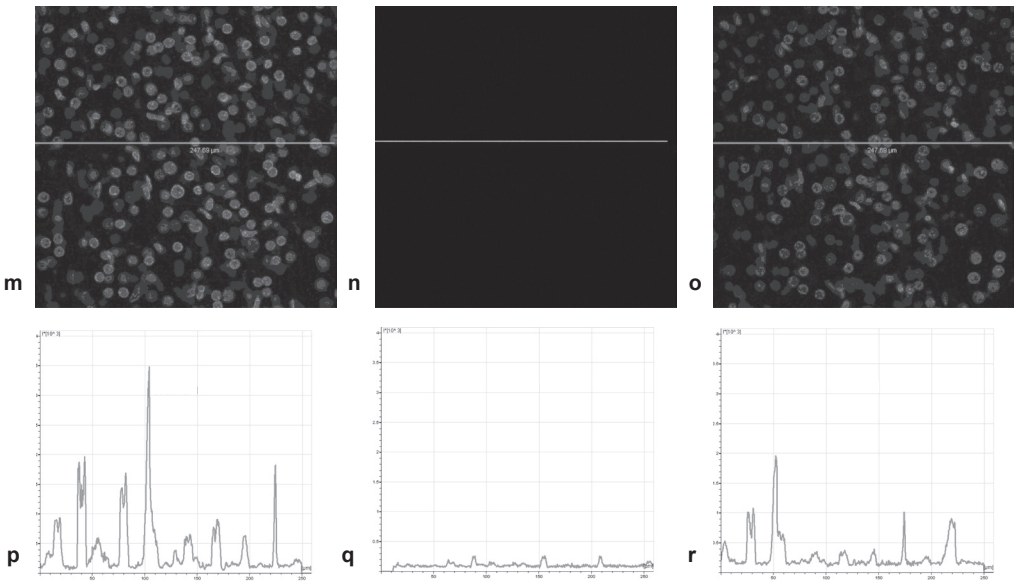

REFERENCES

1. Adolfsson J. Prognostic value of deoxyribonucleic acid content in prostate cancer: a review of current results. Int J Cancer 1994;58:211-216.
2. Bocking A, Stockhause J, Meyer-Ebrecht D. Towards a single cell cancer diagnosis. Multimodal and monocellular measurements of markers and morphology (5M). Cellular Oncology 2004;26:73-79.
3. Rigaut JP, Vassy J, Herlin P, Duigou F, Masson E, Briane D, Foucrier J, Carvajal-Gonzalez S, Downs AM, Mandard AM. 3-dimensional dna image cytometry by confocal scanning laser microscopy in thick tissue blocks. Cytometry 1991;12:511-524.
4. Sapi Z, Hendricks JB, Pharis PG, Wilkinson EJ. Tissue section image analysis of breast neoplasms. Evidence of false aneuploidy. Am J Clin Pathol 1993;99:714-720.
5. Chamgoulov R, Lane P, Macaulay C. Optical computed-tomographic microscope for three-dimensional quantitative histology. Cellular Oncology 2005;26:319-327.
6. Ploeger LS, Huisman A, van der GJ, van der Giezen DM, Belien JA, Abbaker AY, Dullens HF, Grizzle W, Poulin NM, Meijer GA, van Diest PJ. Implementation of accurate and fast DNA cytometry by confocal microscopy in 3D. Cell Oncol 2005;27:225-230.
7. Huisman A, Ploeger LS, Dullens HF, Poulin N, Grizzle WE, van Diest PJ. Development of 3D chromatin texture analysis using confocal laser scanning microscopy. Cell Oncol 2005;27:335-345.
8. Huisman A, Ploeger LS, Dullens HFJ, Belien JA, Meijer GA, Poulin N, Grizzle W, van Diest PJ. Discrimination between benign and malignant prostate tissue using chromatin texture analysis in 3-D by confocal laser scanning microscopy. 2006.
9. Suzuki T, Fujikura K, Higashiyama T, Takata K. DNA staining for fluorescence and laser confocal microscopy. J Histochem Cytochem 1997;45:49-53.
10. Bink K, Walch A, Feuchtinger A, Eisenmann H, Hutzler P, Hofler H, Werner M. TO-PRO-3 is an optimal fluorescent dye for nuclear counterstaining in dual-colour FISH on paraffin sections. Histochemistry and Cell Biology 2001;115:293-299.
11. Bedner E, Du L, Traganos F, Darzynkiewicz Z. Caffeine dissociates complexes between DNA and intercalating dyes: application for bleaching fluorochrome-stained cells for their subsequent restaining and analysis by laser scanning cytometry. Cytometry 2001;43:38-45.
12. Belien JA, van Ginkel AH, Tekola P, Ploeger LS, Poulin NM, Baak JP, van Diest PJ. Confocal DNA cytometry: a contour-based segmentation algorithm for automated three-dimensional image segmentation. Cytometry 2002;49:12-21.
13. Nelder J, Mead R. A simplex method for function minimization. Computer Journal 1965;7:308-313.